ELSEVIER

Journal of Photochemistry and Photobiology A: Chemistry 107 (1997) 125–136

Journal of PHOTOCHEMISTRY AND PHOTOBIOLOGY A:CHEMISTRY

Quenching of aromatic ketone triplet excited states by polysilanes

Ladislau Heisler, Jeanne M. Hossenlopp, Yuping Niu, Mark G. Steinmetz *, Ying Zhang

Department of Chemistry, Marquette University, P.O. Box 1881, Milwaukee, WI 53201-1881, USA

Received 19 August 1996; accepted 25 November 1996

Abstract

Polysilane oligomers quench the triplet excited states of *m*-chlorotrifluoroacetophenone, *p*-chlorotrifluoroacetophenone, *p*-cyanoacetophenone, acetophenone and benzophenone in benzene. The phosphorescence lifetimes τ were measured by laser flash photolysis for varying concentrations of polysilane quencher Q, where $Q \equiv Me_3Si(SiMe_2)_{n-2}SiMe_3$ ($n = 2$–4, 6) and $(Me_2Si)_6$. From τ^{-1} vs. [Q], the bimolecular rate constants for quenching k_q were obtained. Quenching by linear polysilanes Q exhibits a continuous "S-shaped" profile of log k_q vs. ΔG_{et}, the free energy for electron transfer. Limited data indicate a similar, although separate, profile for $(Me_2Si)_6$. In the exergonic region and for ΔG_{et} of less than approximately 7–10 kcal mol^{-1}, log k_q follows the quenching theory via contact ion radical pairs. The regular trend observed in the endergonic region deviates from the theoretical curve and is attributed to a separate mechanism for quenching involving mainly hydrogen atom transfer to form pinacols. As electron transfer becomes favorable, silylated pinacols are observed as the major products of *p*-cyanoacetophenone and tetrasilane ($n = 4$). © 1997 Elsevier Science S.A.

Keywords: Aromatic ketones; Electron transfer; Oligosilanes; Quenching

1. Introduction

Permethylated polysilane oligomers quench the fluorescence of electron-deficient arenes [1–6]. An electron transfer mechanism has been proposed for quenching, consistent with the low oxidation potentials of catenated silanes. For the series of linear oligosilanes $Me_3Si(Me_2Si)_{n-2}SiMe_3$ ($n = 2$–6), the electrochemical oxidation potentials E_{ox} (SCE, CH_3CN) decrease with increasing chain length n ($n = 2$, 1.88 V; $n = 3$, 1.52 V; $n = 4$, 1.33 V, $n = 5$, 1.18 V; $n = 6$, 1.08 V) [7], and the ease of oxidation can be considered to reflect the high energy of the 3s,3p orbitals of silicon and the conjugation of the σ Si–Si bonds along the polysilane chain [8,9]. In one of the reported fluorescence quenching studies [2], the experimental rate constants for quenching, log k_q, were correlated with the theoretical values calculated for quenching by electron transfer as prescribed by Rehm and Weller [10]. This study utilized hexamethyldisilane as the electron donor and a series of substituted benzenes as the photoexcited electron acceptors.

In this paper, we report the quenching results of aromatic ketone triplet excited states by linear permethylated oligosilanes ($n = 2$–4 and 6), and describe limited studies of quenching by the cyclic silane $(Me_2Si)_6$. The reactions of the triplet excited states of acetone, benzophenone and quinones with Me_4Si, $Me_3SiSiMe_3$ and $(Me_3Si)_4Si$ were studied by Alberti et al. [11]. Additional chemically induced dynamic nuclear polarization (CIDNP) studies were reported by Igarashi et al. [12]. The triplet quinones react with $Me_3SiSiMe_3$ and $(Me_3Si)_4Si$ to produce two electron paramagnetic resonance (EPR) detectable quinone radicals [11]. One of these quinone radicals is O-silylated. The other results from the addition of free Me_3Si radicals to a ring carbon of the quinone. In the case of $Me_3SiSiMe_3$, the free Me_3Si radicals may be generated via S_H2 displacement by the triplet quinone. For $(Me_3Si)_4Si$, however, the analogous S_H2 displacement would have to take place at the sterically hindered central silicon. Thus the Me_3Si radicals are thought to be formed, instead, via electron transfer from the hindered silane to the triplet excited quinone, followed by Si–Si bond cleavage of the $(Me_3Si)_4Si$ cation radical. The ΔG_{et} values for electron transfer in acetonitrile were calculated to be exergonic for both $Me_3SiSiMe_3$ and $(Me_3Si)_4Si$ as donors and 2,6-di(tert-butyl)benzoquinone and 9,10-anthraquinone as acceptors.

Our study was prompted by the fact that, in previous work, it was not determined whether the quenching of aromatic ketone triplets by silanes proceeded via electron transfer or via direct S_H2 displacement and/or hydrogen atom abstraction. For triplet benzophenone, the ΔG_{et} (acetonitrile) value was calculated to be endergonic for $Me_3SiSiMe_3$ and ther-

* Corresponding author.

PII S1010-6030(96)04582-0

moneutral for $(Me_3Si)_4Si$ as electron donors [11]. An electron transfer mechanism was not required to account for the phosphorescence quenching of benzophenone or for the observance of EPR signals corresponding to Ph_2C–$OSiMe_3$ and Ph_2C–$OSi(SiMe_3)_3$ radicals. These radical products could have resulted from straight S_H2 displacement. In addition, although Ph_2C–OH radicals from hydrogen abstraction were not observed, the occurrence of this process could not be excluded, since such radicals would have been less persistent than those derived from displacement of silyl. No products of steady state photolysis were reported.

In this paper, we report the rate constants k_q for the phosphorescence quenching of aromatic ketone triplets by $Me_3Si(Me_2Si)_{n-2}SiMe_3$ ($n=2$–4, 6) and $(Me_2Si)_6$ in benzene solvent. When the ΔG_{et} value of the donor–acceptor pair is less than 7–10 kcal mol^{-1}, log k_q correlates with the theoretical values calculated for quenching by the electron transfer mechanism of Rehm and Weller [10]. In the strongly endergonic region, log k_q deviates from theory and shows a separate trend attributable to quenching by direct reaction of the oligosilane quencher with the ketone triplet. This change in the mechanism of quenching is reflected by the major products of steady state photolysis of acetophenone and *p*-cyanoacetophenone with disilane and tetrasilane. Pinacols are major products in the strongly endergonic region, consistent with quenching via direct hydrogen abstraction by the ketone triplet from the oligosilane. When electron transfer is favorable, silylated pinacols are formed, possibly via displacement of silylenium in the contact ion radical pair.

2. Experimental details

The spectra were recorded with the following spectrometers: NMR GE GN 300 (300 MHz ^1H, 75 MHz ^{13}C); Perkin–Elmer 320 (UV). A Hewlett-Packard 5890 GC and an HP 5970 mass-selective detector were used for GC-MS analyses, which were performed at 70 eV with a DB-1 column (0.25 mm × 30 m, 0.25 μm film thickness) temperature programmed at 40 °C for 5 min and then 250 °C at 10 °C min^{-1}. Melting points were determined with a Fisher–Johns melting point apparatus and are uncorrected.

Silica gel (60–200 mesh, grade 62, Mallinckrodt) was used for standard column chromatography. Medium-pressure liquid chromatography (MPLC) utilized an 82 cm × 2.5 cm column of 230–400 mesh silica gel (grade 9385, 60 A, Aldrich) with ether or ethyl acetate in hexane as eluent at a flow rate of 15 ml min^{-1}, as specified below. The column was connected to a Gilson model 305 pump equipped with a 100 ml min^{-1} capacity head, and the eluent was passed through an ISCO UA-5 UV detector.

Analytical separations were performed with Varian 1400 or HP 5720 gas chromatographs using column A (Megabore DB-1 capillary, 0.53 mm × 30 m, 1.5 μm film thickness), column B (Megabore DB-210, 0.53 mm × 30 m, 1.0 μm film thickness) or column C (15 ft × 1/8 in, 5% OV-17 on 100–120 mesh Chromosorb W HP). Nitrogen was used as carrier gas. The flame ionization detector (FID) response was calibrated with standard mixtures, as noted below.

Preparative GC separations were performed on a Gow-Mac Series 580 isothermal gas chromatograph equipped with thermal conductivity detector, utilizing column D (4 ft × 1/4 in, 10% OV-101 on 60–80 mesh Chromosorb W) with He as carrier gas.

The following solvents were used: MeOH (EM Omnisolv, distilled from magnesium), hexanes (Mallinckrodt), benzene (EM OmniSolv, spectrophotometric grade), CH_3CN (Aldrich, HPLC, refluxed over CaH_2 for 3 days and distilled), tetrahydrofuran (THF) (MILSOLV, refluxed over sodium benzophenone and distilled), pentane (Aldrich, spectrophotometric grade), toluene (Aldrich, refluxed for 3 h over CaH_2 and distilled).

The following commercially available compounds were used: butyrophenone (Aldrich, vacuum distilled), acetophenone (Aldrich, vacuum distilled), benzophenone (Aldrich, crystallized from 95% EtOH), *p*-chlorotrifluoroacetophenone (Aldrich, vacuum distilled), *p*-cyanoacetophenone (Aldrich, crystallized from 95% ethanol), hexamethyldisilane (PCR, distilled). The purity was established by GC-MS.

Known compounds were prepared by minor modifications of literature procedures. *m*-Chlorotrifluoroacetophenone [13] was synthesized by the literature procedure [14], modified by substituting lithium trifluoroacetate for trifluoroacetic acid; purification was by standard column chromatography, eluting with ethyl acetate in hexanes. *p*-Cyanobutyrophenone was synthesized by the procedure reported for *p*-cyanovalerophenone [15]; recrystallization from hexane gave material (m.p., 46–47 °C) with satisfactory elemental analysis. Dodecamethylcyclohexasilane [16,17] was crystallized from acetone in hexane, m.p. 251–253 °C (m.p. 250–252 °C [16]).

2.1. Octamethyltrisilane [18]

The trisilane was synthesized by the literature procedure [18] from 15 g (2.1 mol) of lithium wire (Aldrich), 180 g (1.7 mol) of chlorotrimethylsilane (Aldrich) and 65 g (0.52 mol) of dichlorodimethylsilane (Aldrich). Fractional distillation of the crude product through a 15 cm Vigreaux column gave 23 g, b.p. 145–178 °C. Redistillation through a 20 cm × 1 cm column of steel wool gave 14 g (13% yield) of NMR pure octamethyltrisilane, b.p. 170–178 °C (b.p. 175–176 °C [19]). Standard 90 cm × 2.5 cm column chromatography, eluting with hexane and taking 35 ml fractions, gave the product in fractions 9–11. Preparative GC on column D (130 °C) then gave 5.2 g of 99% octamethyltrisilane according to GC-MS analysis. The spectral data were as follows: ^1H NMR ($CDCl_3$) δ: 0.06 (s, 6 H, methyl), 0.07 (s, 18 H, methyl); GC-MS *m/z* (relative intensity): 204 (5), 189 (5), 132 (5), 131 (29), 116 (20), 115 (7), 101 (7), 75 (4), 74 (8), 73 (100), 59 (11), 45 (42), 44 (6), 43 (20).

2.2. Decamethyltetrasilane [19]

The tetrasilane was prepared from 41 g (0.24 mol) of chloropentamethyldisilane [20] and 15.0 g (0.652 mol) of sodium following the literature method [19]. The crude product, containing minor amounts of tetradecamethylhexasilane and other byproducts, was fractionally distilled through a 20 cm Vigreaux column to give 14 g, b.p. 55–62 °C (0.2 mmHg). A volatile impurity of b.p. 25–35 °C (0.3 mmHg) was removed by distillation through a 14 cm column packed with cut glass tubing, and MPLC of the residue on a 30 cm ×2.5 cm column, eluting with hexane and taking 35 ml fractions, gave 8.7 g (38% yield based on chloropentamethyldisilane) of 99% product in fractions 3–5, according to GC-MS analysis. The spectral data were as follows: ^{1}H NMR ($CDCl_3$) δ: 0.06 (s, 18 H, methyl), 0.08 (s, 12 H, methyl); GC-MS *m/z* (relative intensity): 262 (10.5), 247 (2.8), 190 (5), 189 (20), 174 (8), 173 (12), 159 (5), 132 (7), 131 (39), 129 (9), 116 (21), 115 (12), 101 (6), 99 (5), 74 (9), 73 (100), 59 (13), 45 (34), 43 (13).

2.3. Tetradecamethylhexasilane [21,22]

To 7.0 g of approximately 80% pure 1,6-dichlorododecamethylhexasilane (13 mmol of dichloride) [21] and 100 ml of dry THF was added 20 ml (60 mmol) of 3 M methyl magnesium bromide in ether via a syringe with cooling in an ice bath. After reflux overnight, saturated NH_4Cl was added. The aqueous phase was extracted with 100 ml of pentane, and the combined extracts were washed twice with 50 ml of water, dried over anhydrous Na_2SO_4 and concentrated in vacuo. MPLC on a 30 cm×2.5 cm column with hexane as eluent, taking 20 ml fractions, gave 4.4 g of 95% pure product by GC-MS analysis in fractions 6–8. Preparative GC on column D (185 °C) gave 2.4 g (49% yield) of 99% tetradecamethylhexasilane, m.p. 29–30.5 °C (m.p. 28–29 °C [22]). The spectral data were as follows: ^{1}H NMR ($CDCl_3$) δ: 0.09 (s, 18 H, methyl), 0.13 (s, 12 H, methyl), 0.17 (s, 12 H, methyl); GC-MS *m/z* (relative intensity): 378 (18), 363 (2), 247 (9), 189 (12), 174 (16), 173 (27), 131 (15), 73 (100), 45 (22).

2.4. 2,3-Di(p-cyanophenyl)-2,3-butanediol

A solution of 5.0 g (0.034 mol) of *p*-cyanoacetophenone (Aldrich) and 10 drops of glacial acetic acid in 250 ml of 2-propanol was purged for 1 h with nitrogen, and then irradiated for 3 h with a Hanovia 450 W medium-pressure mercury lamp equipped with a uranium filter ($\lambda > 330$ nm), as prescribed in the literature for acetophenone pinacol [23]. A colorless precipitate formed, which was filtered and dried in vacuo for 24 h to give 1.8 g (36% yield) of colorless crystals of *d,l*- and *meso*-*p*-cyanoacetophenone pinacol, m.p. 258–259 °C. The *d,l* and *meso* assignments were made according to the literature [24]. The spectral data were as follows: ^{1}H NMR ($(CD_3)_2SO$) δ: 1.22 and 1.60 (each s, 6 H combined integral, methyls, 9 : 1 *d,l* : *meso*), 5.37 and 5.55 (each s, 2 H combined integral, hydroxyl), 7.23 (d, $J = 8.3$ Hz, A part of AA'BB', aromatic, *meso*), 7.50 (d, $J = 8.3$ Hz, B part of AA'BB', aromatic *meso*), 7.67 (d, $J = 8.3$ Hz, A part of AA'BB', aromatic, *d,l*), 7.74 (d, $J = 8.3$ Hz, B part of AA'BB', aromatic, *d,l*), combined integral of aromatics of 8 H; ^{1}H NMR ($(CD_3)_2CO$) δ: 1.45 and 1.72 (each s, 6 H combined integral, methyls, 9 : 1 *d,l* : *meso*), 4.54 and 4.72 (s, 2 H combined integral, hydroxyl), 7.38 (d, $J = 8.8$ Hz, A part of AA'BB', aromatic, *meso*), 7.48 (d, $J = 8.8$ Hz, B part of AA'BB', aromatic, *meso*), 7.65 (d, $J = 8.8$ Hz, A part of AA'BB', aromatic, *d,l*), 7.75 (d, $J = 8.8$ Hz, B part of AA'BB', aromatic, *d,l*), combined integral of aromatics of 8 H; ^{13}C NMR ($(CD_3)_2SO$) δ: 24.4, 24.6, 76.7, 77.0, 108.6, 108.9, 119.2, 127.9, 128.7, 130.1, 130.6, 152.0, 152.4. Analysis: calculated for $C_{18}H_{16}N_2O_2$: C, 73.96%; H, 5.52%; N, 9.58%; found: C, 73.84%; H, 5.49%; N, 9.49%.

2.5. 2,3-Di(p-cyanophenyl)-2,3-butanediol monotrimethylsilyl ether

The half-silylated *p*-cyanoacetophenone pinacol was synthesized following a literature silylation procedure [25]. To a mixture of 20 ml of dry THF, 0.21 g (0.72 mmol) of *p*-cyanoacetophenone pinacol (9 : 1 diastereomeric mixture) and 0.20 g (2.0 mmol) of triethylamine, cooled in an ice bath, was added (dropwise via a syringe) 0.21 g (1.9 mmol) of chlorotrimethylsilane. The mixture was refluxed for 46 h, followed by the addition of 20 ml of water and extraction twice with 40 ml of ether. The combined extracts were washed twice with 20 ml of water, dried over anhydrous Na_2SO_4 and concentrated in vacuo to give 64 mg of a yellow solid, which was further purified by MPLC using 10% ethyl acetate in hexanes as eluent. The peak collected at 72 min retention time gave 51 mg of *p*-cyanoacetophenone mono(trimethylsilyl) pinacol. Crystallization from ether in pentane (1 : 1, v/v) afforded 32 mg (12% yield) of colorless needles, m.p. 167–168 °C. The spectral data were as follows: ^{1}H NMR ($(CD_3)_2CO$) δ: −0.05 (s, 9 H, methyl), 1.38 (s, 3 H, methyl), 1.51 (s, 3 H, methyl), 4.47 (s, 1 H, hydroxyl, exchanged with D_2O), 7.70–7.78 (m, 8 H, aromatic); ^{13}C NMR ($CDCl_3$) δ: 2.0, 23.6, 24.8, 78.3, 81.4, 110.7, 110.9, 118.7, 118.9, 128.1, 128.2, 130.9, 149.1, 149.6. Analysis: calculated for $C_{21}H_{24}N_2O_2Si$: C, 69.20%; H, 6.64%; N, 7.68%: found: C, 69.09%; H, 6.69%; N, 7.61%.

2.6. Exploratory photolyses of acetophenone with $Me_3SiSiMe_3$ and $Me_3Si(SiSe_2)_2SiSe_3$ in benzene

A solution of 0.1 M of acetophenone in 25 ml of 0.3 M $Me_3SiSiMe_3$ or 0.2 M $Me_3Si(Me_2Si)_2SiMe_3$ in benzene was purged with nitrogen and irradiated through a uranium filter ($\lambda > 330$ nm) with a Hanovia 450 W medium-pressure lamp. The photolyses were monitored by GC-MS. The major product of both oligosilanes was a 1 : 1 diastereomeric mixture of acetophenone pinacols, identified by comparison of their

retention times and GC-MS data with an authentic sample [23,24]. Authentic samples of 1-phenethyl alcohol (Aldrich) and its trimethylsilyl ether derivative, prepared by a standard silylation procedure [25], were used to identify these minor products in the photomixtures.

In the order of their retention times, the GC-MS data of the products of photolysis with $Me_3SiSiMe_3$ were as follows: $PhSiMe_3$ (10.7 min) *m/z* 150 (9), 136 (15), 135 (100), 107 (8), 105 (10), 53 (11), 43 (31); $PhCH(OSiMe_3)Me$ (13.2 min), *m/z* no parent, 193 (1), 180 (11), 179 (64), 105 (15), 77 (20), 75 (100), 74 (16), 73 (71), 47 (13), 45 (27), 43 (14); $PhCH_2SiMe_2SiMe_3$ (16.5 min) *m/z* 222 (15), 207 (12), 149 (37), 148 (11), 133 (10), 132 (14), 131 (86), 121 (33), 91 (11), 73 (100), 65 (10), 59 (13), 45 (49), 43 (39); biphenyl (16.6 min) *m/z* 154 (100), 153 (45), 152 (31), 151 (11), 77 (11), 76 (21), 75 (10), 74 (10), 63 (12), 51 (16), 50 (11); $(Me_5Si_2)CH_2CH_2$-(Si_2Me_5) (16.8 min) *m/z* 290 (7), 275 (2), 217 (20), 143 (13), 131 (27), 117 (12), 73 (100), 59 (15), 45 (26), 43 (10); unidentified (21.7 min) *m/z* 264 (44), 249 (8), 191 (10), 133 (13), 132 (15), 131 (86), 75 (13), 74 (10), 73 (100), 59 (12), 45 (38), 43 (60); acetophenone pinacols, 1 : 1 ratio of diastereomers (23.1 min and 23.2 min) *m/z* no parent, 122 (12), 121 (22), 107 (3), 105 (4), 78 (5), 77 (8), 51 (6), 43 (100); mono(trimethylsilyl) pinacols, 1 : 1 ratio of diastereomers (23.6 min and 23.8 min) *m/z* no parent, 299 (3), 194 (15), 193 (70), 177 (6), 77 (10), 75 (19), 74 (9), 73 (100), 45 (17), 43 (55). 1-Phenethyl alcohol, which was obscured by acetophenone, was detected on column B (65 °C). Other minor products were observed but not identified.

The photolysis with $Me_3(SiMe_2)_2SiMe_3$ gave, in addition to the above products, the following: $PhSiMe_2SiMe_3$ (15.1 min) *m/z* 208 (8), 193 (6), 136 (9), 135 (100), 107 (7), 105 (9), 73 (28), 69 (8), 45 (17), 43 (24); diastereomeric mono(pentamethyldisilanyl) pinacol (26.4 min and 26.6 min) *m/z* no parent, 357 (5), 300 (8), 299 (27), 252 (9), 251 (55), 177 (11), 133 (21), 131 (89), 121 (7), 75 (76), 73 (98), 45 (27), 43 (100); two $(Me_9Si_4)CH_2CH_2(Si_4Me_9)$ isomers (28.2 min and 28.8 min) with similar fragmentation patterns, *m/z* 522 (19), 247 (22), 245 (52), 190 (16), 173 (24), 131 (40), 73 (100), 45 (12); diastereomeric mono(heptamethyltrisilanyl) pinacols (30.1 min and 30.4 min) *m/z* no parent, 357 (7), 309 (49), 299 (64), 208 (11), 189 (56), 177 (13), 133 (16), 131 (36), 129 (24), 115 (13), 91 (13), 75 (82), 73 (100), 45 (24), 43 (96). Numerous other minor products were formed, but not identified.

2.7. *Exploratory photolysis of p-cyanoacetophenone with 0.6 M $Me_3SiSiMe_3$ in benzene*

A solution of 0.040 M *p*-cyanoacetophenone (10.1 mmol) in 25 ml of 0.60 M $Me_3SiSiMe_3$ in benzene was purged with nitrogen and then irradiated for 5 h through a uranium filter with a Hanovia 450 W medium-pressure lamp. Concentration in vacuo afforded a colorless precipitate, which was filtered and dried in vacuo to give 95 mg (0.32 mmol, 6.4% yield) of *p*-cyanoacetophenone pinacols (1 : 1 diastereomers according to ^1H NMR integration) with m.p. 259–262 °C. The diastereomeric pinacol was identified by comparison of the ^1H and ^{13}C NMR ($(CD_3)_2SO$) spectra with those of an authentic sample and by the mixture m.p. 262–263 °C. After complete precipitation of pinacol and further concentration of the photolysate to dryness, 1.3 g of a yellow solid was obtained. ^1H NMR showed starting ketone and minor products, which were isolated by MPLC, eluting initially with 10% ethyl acetate in hexanes and gradually increasing the ethyl acetate to 20%. The first and third peaks at 24 min and 42 min retention times gave 4 mg and 8 mg of unidentified products. The second peak at 30 min retention time gave 8 mg (0.02 mmol, 0.4% yield) of *p*-cyanoacetophenone bis(trimethylsilyl) pinacol (1 : 1 diastereomers by ^1H NMR), which was fully characterized spectroscopically. A cut at 75 min retention time at the onset of the fourth peak gave 12 mg (0.033 mmol, 0.66% yield) of *p*-cyanoacetophenone mono(trimethylsilyl) pinacol, identified from a comparison with an authentic sample. The remainder of the fourth peak centered at 80 min retention time gave 1.3 g (8.8 mmol, 87% recovery) of unreacted ketone. The percentage yields for all pinacols (unsilylated, monosilylated and bissilylated) were calculated on the basis of 2 mmol *p*-cyanoacetophenone consumed per millimole of product formed.

The spectral data for *p*-cyanoacetophenone bis(trimethylsilyl) pinacol were as follows: ^1H NMR ($(CD_3)_2CO$) δ: −0.09 (each s, 18 H combined integral, Si methyls, 1 : 1 *d,l* : *meso*), 1.45 and 1.87 (each s, 6 H combined integral, methyls, 1 : 1 *d,l* : *meso*), 7.11, 7.47 and 7.79 (each m, 8 H combined integral, aromatic); ^1H NMR ($CDCl_3$) δ: −0.13 and 0.06 (each s, 18 H combined integral, methyls, 1 : 1 *d,l* : *meso*), 1.36 and 1.79 (each s, 6 H combined integral, methyls, 1 : 1 *d,l* : *meso*), 6.92, 7.33 and 7.62 (each m, 8 H combined integral, aromatic); ^{13}C NMR ($CDCl_3$) δ: 1.9, 2.0, 23.2, 23.7, 81.8, 81.5, 110.3, 110.6, 118.9, 119.0, 128.2, 128.7, 129.9, 130.7, 150.1, 150.9. HR MS (M^+ not observed, $M^+ - CH_3$, $C_{23}H_{29}N_2O_2Si_2$): calculated: 421.1768; found: 421.1764.

GC-MS analyses showed numerous minor volatile products, including $PhSiMe_3$ and $(Me_5Si_2)CH_2CH_2(Si_2Me_5)_2$ at 10.4 min and 16.8 min retention times. Additional products, reported according to (retention time) *m/z* (relative intensity) were as follows: $(p\text{-}NCPh)CH(OSiMe_3)Me$ (17.9 min), 219 (3), 204 (30), 130 (6), 103 (8), 75 (100), 73 (52), 45 (20), 43 (12);.trimethylsilyl enol ether of starting ketone (19.0 min) 217 (17), 216 (22), 202 (41), 160 (21), 128 (6), 116 (6), 101 (11), 77 (13), 75 (100), 73 (47), 47 (24), 45 (41); unidentified disilane addition product of *p*-cyanoacetophenone (23.9 min) 291 (2), 276 (2), 218 (8), 216 (13), 147 (5), 133 (9), 75 (100), 73 (93), 59 (7), 45 (34), 43 (23); unidentified disilane addition product of *p*-cyanoacetophenone (25.1 min) 291 (9), 276 (2), 216 (15), 205 (5), 147 (83), 131 (12), 117 (10), 75 (14), 73 (100),

45 (29). The pinacols are non-volatile and thus are not detected by GC-MS.

2.8. Exploratory photolysis of p-cyanoacetophenone in 0.03 M $Me_3Si(SiMe_2)_2SiMe_3$ in benzene

A solution of 1.3 g (9.1 mmol, 0.036 M) of *p*-cyanoacetophenone and 2.2 g (8.5 mmol, 0.034 M) of tetrasilane in 250 ml of benzene was purged with nitrogen and then irradiated as above for 3 h, monitoring by ^{1}H NMR spectroscopy. Concentration in vacuo gave 3.1 g of a yellow oil, which ^{1}H NMR spectroscopy showed to be *p*-cyanoacetophenone, tetrasilane and a mixture of bis(polysilanyl) pinacols. Unsilylated pinacol was very minor, and half-silylated pinacol was not detected on the basis of comparisons with authentic pinacol and mono(trimethylsilyl) pinacol. MPLC, eluting with 5% ethyl acetate in hexanes and gradually increasing the concentration of ethyl acetate to 20%, gave 1.4 g (62% recovery, 3.2 mmol reacted) of tetrasilane in peak 1 at 25 min retention time. The second peak at 50 min retention time gave 1.05 g of a mixture of *p*-cyanoacetophenone bis(polysilanyl) pinacols. The third peak at 75 min retention time gave 0.28 g (21.2% recovery, 7.2 mmol reacted) of *p*-cyanoacetophenone. The spectral data of the diastereomeric bis(polysilanyl) pinacols were as follows: ^{1}H NMR ($CDCl_3$) δ: from −0.19 to 0.26 (cluster of singlets, 24 H, Si methyls), 1.34–1.37 and 1.77–1.79 (two clusters of singlets, 6 H combined integral, methyls, approximately 1 : 1 diastereomers), 6.91–6.93, 7.31–7.34 and 7.57–7.64 (several m, 8 H, aromatic); ^{1}H NMR ($(CD_3)_2CO$) δ: from −0.13 to 0.13 (several s, 24 H, Si methyls), 1.45–1.50 and 1.86–1.87 (several s, 6 H, methyl, approximately 1 : 1 diastereomers), 7.11–7.18, 7.50–7.56 and 7.72–7.83 (several m, 8 H, aromatic, diastereomers); ^{13}C (APT) NMR ($CDCl_3$) δ: −2.1, −1.7, −1.6, 1.5, 1.6, 1.7, 1.9, 2.0 ($\underline{C}H_3$–Si); 23.2, 23.3, 23.5, 23.8, 23.9 ($\underline{C}H_3$–C–O); 81.1, 81.2, 81.5, 81.6, 81.9 (Ar–$\underline{C}$–O); 110.3, 110.4, 110.5, 110.7, 110.8 (aromatic $\underline{C}$–CN); 118.9 (Ar–$\underline{C}$N); 128.2, 128.3, 128.4, 128.7, 128.8, 130.0, 130.6, 130.7 (aromatic $\underline{C}$H); 150.1, 150.2, 150.9 (aromatic $\underline{C}$–C–O); ^{13}C NMR ($(CD_3)_2SO$) δ: −2.1, −1.7, 1.4, 1.5, 1.8, 1.9, 2.9, 23.1, 23.3, 23.5, 23.7, 80.8, 81.2, 81.3, 81.6, 81.8, 109.3, 109.4, 109.5, 109.7, 109.8, 118.8, 118.9, 128.3, 128.4, 128.7, 128.8, 130.1, 130.8, 150.1, 150.5, 150.6; IR (neat): 3.34, 3.39, 3.45, 4.49, 5.22, 6.66, 7.12, 7.31, 7.99, 8.24, 8.70, 9.00, 9.82, 10.18, 10.36, 11.86, 12.43, 12.80, 13.12, 13.79 μm. The HETCOR NMR data are summarized in Section 3.

Numerous minor volatile products were observed by GC-MS analysis of the photolysate prior to MPLC, including $PhSiMe_3$ at 10.7 min retention time, (*p*-NCPh)CH(OSiMe$_3$)Me at 18.1 min and trimethylsilyl enol ether of the ketone at 19.2 min, as reported above for the disilane. The GC-MS data as (retention time) m/z of the additional minor products were as follows: (*p*-NCPh)CH(OSi$_2$Me$_5$)Me (20.5 min) 277 (13), 262 (41), 204 (76), 160 (28), 147 (40), 130 (62), 102 (63), 73 (100), 45 (64); (*p*-NCPh)C(OSi$_2$Me$_5$)=CH$_2$ (22.2 min) 275 (4), 260 (12), 202 (9), 160 (8), 147 (80), 133 (9), 101 (9), 75 (61), 73 (100), 59 (11), 45 (49); unidentified (23.2 min) 351 (2), 336 (5), 278 (52), 130 (100), 102 (34), 73 (22), 45 (13); (*p*-NCPh)CH(OSi$_3$Me$_7$)Me (24.1 min) 335 (3), 278 (4), 205 (33), 147 (28), 130 (17), 117 (22), 103 (11), 75 (52), 73 (100), 45 (30); (*p*-NCPh)C(OSi$_3$Me$_7$)=CH$_2$ (25.1 min) 333 (7), 318 (4), 260 (60), 202 (3), 191 (3), 147 (8), 131 (13), 101 (8), 75 (30), 73 (100), 45 (33).

2.9. Quantum yield determinations

A semi-micro-optical bench for quantum yield determinations was constructed along the lines reported previously [26,27]. Light output was determined by ferrioxalate actinometry [28] using the splitting ratio technique [27]. All photolysates were purged with nitrogen for 1 h prior to and during irradiation. Solutions of 0.01 M ketone and various concentrations of oligosilane quencher in 40 ml of benzene were irradiated at 340 nm.

With acetophenone plus oligosilane, the starting materials, pinacol, half-silylated pinacols and biphenyl were quantified on column A, programmed at 100 °C for 20 min, 120 °C for 15 min and then 165 °C, with *n*-heptadecane as internal standard for calibration of the detector response. The quantum yields of pinacol were corrected by 8%–10% for hydrogen abstraction from the solvent by subtracting the amount of biphenyl formed. The trimethylsilyl derivative of 1-phenethyl alcohol was quantified separately on column A (85 °C) with *n*-dodecane standard, and 1-phenethyl alcohol was quantified on column B (65 °C) with *n*-tridecane standard.

With *p*-cyanoacetophenone and the oligosilanes, GC column C, programmed at 60 °C for 8 min and then 180 °C at 8 °C min^{-1}, was used to quantify the reactants, whereas ^{1}H NMR (acetone-d_6) spectroscopy was used to quantify the products. Diphenylmethane was used as an NMR standard; no correction of the integrated peak areas against the standard was necessary, as found from a calibration curve constructed for known mixtures of pinacol plus standard.

For both acetophenone and its *p*-cyano derivative, the quantum yields of pinacols and half-silylated pinacols were calculated on the basis of 1 mmol of product per 2 millieinstein absorbed, whereas the quantum yields of all other products assume 1 mmol of product per 1 millieinstein absorbed. With *p*-cyanoacetophenone, the concentrations of the oligosilanes were adjusted to achieve half-quenching, such that $\tau^{-1} = k_q[Q]$, where τ is the lifetime of the triplet ketone at room temperature in fluid solution in the absence of quencher. Acetophenone quantum yields at various concentrations of disilane were measured to obtain Stern–Volmer quenching constants $k_q\tau$ from linear regression analysis. From the measured τ values (see below), the quantum yields at half-quenching were calculated.

The quantum yields of Norrish type II reaction of butyrophenone and *p*-cyanobutyrophenone at various concentrations of oligosilanes in benzene, MeOH and CH_3CN were determined by methods similar to those described for aceto-

phenone. For GC analyses, the detector response was calibrated with known mixtures.

2.10. Phosphorescence lifetime experiments

Triplet lifetimes were determined from monoexponential fits of the phosphorescence decays of solutions of acetophenone (AC), benzophenone (BP), *p*-cyanoacetophenone (CNA), *p*-chlorotrifluoroacetophenone (PCFA) and *m*-chlorotrifluoroacetophenone (MCFA) in benzene containing various concentrations of oligosilanes $Me_3Si(SiMe_2)_{n-2}SiMe_3$ ($n=2$–4, 6) and $(Me_2Si)_6$ as quenchers. The solutions of 0.02 M ketone and 0–0.5 M quencher were freshly prepared and degassed by three freeze–pump–thaw cycles in long-necked 1 cm square quartz cells and kept under vacuum for all determinations. The phosphorescence decays were determined at an emission wavelength of 450 nm (293 K), except for MCFA, where $\lambda_{em}=440$ nm. Excitation was at 340 nm and employed a Lambda Physik dye laser (*p*-terphenyl in dioxane), pumped by a pulsed (50 ns) Questek 2720 XeCl excimer laser [29]. Laser energies ranged from 0.1 to 3 mJ and were monitored by a Molectron J-25 joule meter. The emission from the center of the cell was collected 90° to the incident laser beam and focused by a cylindrical lens onto the entrance slit of a PTI 1/4 m monochromator. Phosphorescence was detected by a Hamamatsu model R1104 photomultiplier tube. A Le Croy 9410 digital oscilloscope was used for transient signal acquisition and averaging. The final time-resolved phosphorescence decay signal (average of 100 transient signals) was transferred to a Northgate 386 computer for data processing and linear regression analysis to give the $k_d=\tau^{-1}$ values. Stern–Volmer linear correlations of τ^{-1} vs. [oligosilane] gave slopes of k_q, the quenching rate constant. All experiments were performed at 293 K.

3. Results

3.1. Quenching of the Norrish type II photoreaction by oligosilanes

The longer chain oligosilanes in the series $Me_3Si(SiMe_2)_{n-2}SiMe_3$ ($n=2$–4, 6) [30,31] and $(Me_2Si)_6$ [30] have ionization potentials (I_p, Table 1) approaching that of triethylamine (7.50 eV), suggesting the possibility that these oligosilanes, like the amines [32], may quench the triplet excited states of aromatic ketones, including the short-lived n,π* triplet (0.133 μs [33]) of butyrophenone. Benzene was used as the solvent, since oligosilanes with $n\geq 4$ show limited solubility in acetonitrile. In the absence of added oligosilane, the quantum yield of the Norrish type II reaction to give acetophenone was found to be identical with the previously reported value for benzene as the solvent ($\Phi^o=0.36$ [33]); the minor phenylcyclobutanol product ($\Phi^o=0.042$ [33]) was not determined. Quenching was only observed for oligosilanes with $n\geq 4$ and for $(Me_2Si)_6$. For these cases, the quantum yields were determined as a function of the oligosilane concentration. The Stern–Volmer slopes $k_q\tau$ from plots of Φ^o/Φ vs. [oligosilane] were small (Table 1), and k_q never exceeded 10^7 M^{-1} s^{-1}. With the tetrasilane, a change in solvent from benzene to methanol resulted in an increase in $k_q\tau$ of approximately eightfold from 0.18 to 1.5. Without quencher, Φ^o(photoelimination) = 0.72–0.83 in pure methanol.

Table 1
Quenching of the Norrish type II photoelimination by oligosilanes $Me_3(SiMe_2)_{n-2}SiMe_3$ and $(Me_2Si)_6$

Quencher	I_p (eV)	$k_q\times 10^6$ (M^{-1} s^{-1}) [a] ($k_q\tau$ (M^{-1}))	
		$PhCOCH_2CH_2CH_3$	*p*-$CNPhCOCH_2CH_2CH_3$
$n=3$	8.19	n.d.	1.5±0.2 (0.45±0.06)
$n=4$	7.29	1.38±0.03 (0.18±0.08)	16±2 (4.9±0.5)
$n=6$	7.02	2.70±0.05 (0.35±0.02)	160±20 (49±7)
$(Me_2Si)_6$	7.29	2.6±0.04 (0.34±0.06)	4.2±0.4 (1.25±0.08)

[a] Calculated from $k_q\tau$ using $\tau=0.133$ μs (butyrophenone) from Ref. [33] or $\tau=0.3$ μs, which is the average lifetime calculated from $k_q\tau$ using k_q of *p*-cyanoacetophenone for $n=3$, 4 and 6 and $(SiMe_2)_6$ as described in the text.

Since quenching of the short-lived n,π* triplet of butyrophenone by oligosilanes was inefficient, we examined the quenching of *p*-cyanobutyrophenone which, like *p*-cyanovalerophenone [15], was expected to have a less reactive lowest energy π,π* triplet with respect to intramolecular hydrogen abstraction. Quenching of the Norrish type II photoelimination of *p*-cyanobutyrophenone by oligosilanes ($n\geq 3$) was more efficient than for butyrophenone (Table 1), and quenching by the tetrasilane was sevenfold more efficient in methanol ($k_q\tau=34\pm 3$ M^{-1}) than in benzene ($k_q\tau=4.9\pm 0.5$ M^{-1}). The quantum yields were Φ^o(MeOH) = 0.56–0.59 and Φ^o(benzene) = 0.16–0.20, and plots of Φ^o/Φ vs. [oligosilane] in benzene are shown in Fig. 1. The rate constants for quenching (k_q) were calculated from an estimated lifetime of $\tau=0.3$ μs (Table 1). This estimate corresponds to the average lifetime obtained by dividing the experimental $k_q\tau$ values for the quenching of *p*-cyanobutyrophenone by the k_q values obtained from the quenching of the phosphorescence of *p*-cyanoacetophenone (see below). The estimated lifetime of 0.3 μs, compared with 0.13 μs for butyrophenone, is in good agreement with the measured difference of approximately a factor of two in the lifetimes for valerophenone and *p*-cyanovalerophenone in benzene [15].

A plot of log k_q vs. I_p of the quencher (Fig. 2) curves upwards with increasing ease of oxidation of the oligosilane. The curvature suggests the possibility of a change in the mechanism of quenching as electron transfer from the oligosilane electron donor becomes more favorable. Diffusion-

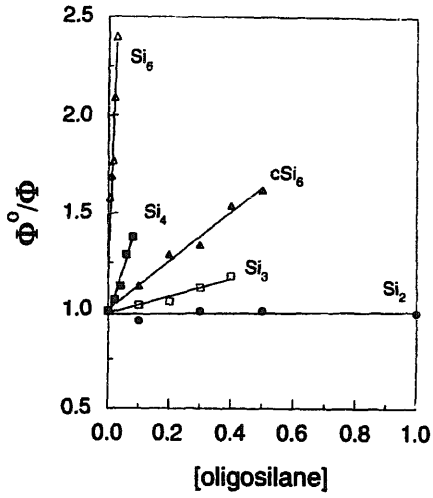

Fig. 1. Φ^{o}/Φ vs. [oligosilane] for quenching of the Norrish type II photoelimination of *p*-cyanobutyrophenone in benzene.

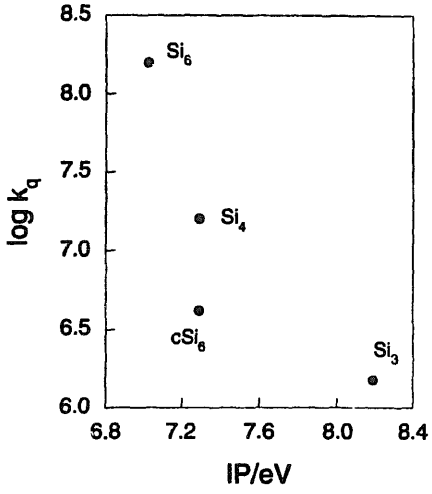

Fig. 2. Correlation of log k_q vs. I_p of oligosilane in the quenching of the Norrish type II photoelimination of *p*-cyanobutyrophenone in benzene.

controlled quenching also appears to be achievable if stronger ketone acceptors are employed. We explored these points by studying the phosphorescence quenching of a series of ketone acceptors.

3.2. Phosphorescence quenching

The linear oligosilanes $Me_3Si(SiMe_2)_{n-2}SiMe_3$ (n = 2–4, 6) were found to quench the transient phosphorescence of AC, BP, CNA, PCFA and MCFA in benzene as solvent. Quenching of the phosphorescence of CNA and AC was also examined with the cyclic silane $(Me_2Si)_6$. Tables 2 and 3 summarize the rate constants k_q for quenching, which were obtained from the slopes of plots of τ^{-1} vs. the concentration of the quencher (Figs. 3–5).

The log k_q values of each donor-acceptor pair are plotted against the free energy for electron transfer (ΔG_{et}) in benzene (Fig. 6). The limited data (Table 3) for quenching by $(Me_2Si)_6$ are omitted for clarity, but appear to follow a similar, although separate, trend as the linear oligosilanes. The full curve in Fig. 6 corresponds to the theory for quenching by the electron transfer mechanism of Rehm and Weller [10] (Section 4). Since electron transfer to form solvated ion radical pairs will not be significant in benzene, the ΔG_{et} values were calculated for contact ion radical pairs (CIRPs), i.e. exciplexes, using Eq. (1) [35], which employs the redox potentials of the ketones [34] and the oligosilanes [35,36] measured in acetonitrile vs. SCE

$$\Delta G_{et}(\text{eV}) = (E_{ox} - E_{red})_{37} - E_T - \frac{\mu^2}{r^3}\left(\frac{\epsilon_s + 1}{2\epsilon_s - 1} - 0.186\right) + 0.38 \quad (1)$$

The dipole stabilization term (benzene ϵ_s = 2.28) in Eq. (1) is estimated to be negligible. Since the electrochemical oxidations of oligosilanes are not reversible [7,11], the ΔG_{et} values can only be considered to be approximate. Alberti et al. [11] have noted that the oxidation potentials represent the upper limits for E_{ox}, which would mean that the actual ΔG_{et} values may be more negative than the values given in Tables 2 and 3.

3.3. Product studies

The major photoproducts of acetophenone and *p*-cyanoacetophenone with the disilane ($Me_3SiSiMe_3$) and tetrasilane ($Me_3Si(SiMe_2)_2SiMe_3$) in benzene were identified to be pinacols or silylated derivatives of pinacols. Significant fractions of ketone and oligomeric silane were consumed to form other, non-pinacolic products, the most important of which were silyl enol ethers and O-silylated arylethanols (see Section 2). These apparent disproportionation products of silylated ketyl radicals may reflect substantial steric hindrance of the recombination pathway. The silyl enol ethers may also be

Table 2
ΔG_{et} from Eq. (1) and k_q for phosphorescence quenching of *m*-chlorotrifluoroacetophenone (MCFA) and *p*-chlorotrifluoroacetophenone (PCFA) in benzene [a]

Acceptor [b]	Silane donor	E_{ox} (V)	ΔG_{et} (kcal mol^{-1})	k_q (10^5 M^{-1} s^{-1})
MCFA	n=4	1.33	−0.922	9220 ± 1800
MCFA	n=6	1.08	−6.69	105000 ± 35000
PCFA	n=2	1.88	15.0	7.17 ± 1.5
PCFA	n=4	1.33	2.30	2460 ± 340
PCFA	n=6	1.08	−3.46	29800 ± 3500

[a] Redox potentials vs. SCE in acetonitrile from Refs. [7,34]; E_T from 0,0 band of phosphorescence in methyltetrahydrofuran [34].
[b] MCFA, E_{red} = −1.25 V, E_T = 69.2 kcal mol^{-1} [34]; PCFA, E_{red} = −1.32 V, E_T = 67.6 kcal mol^{-1} [34].

Table 3
ΔG_{et} from Eq. (1) and k_q for phosphorescence quenching of *p*-cyanoacetophenone (CNA), acetophenone (AC) and benzophenone (BP) in benzene [a]

Acceptor[b]	Silane donor	E_{ox} (V)	ΔG_{et} (kcal mol^{-1})	k_q (10^5 M^{-1} s^{-1})
CNA	$n=2$	1.88	19.4	3.53±0.22
CNA	$n=3$	1.52	11.1	10.9±0.5
CNA	$(Me_2Si)_6$	1.45	9.45	114±9
CNA	$n=4$	1.33	6.69	86.9±9.1
CNA	$n=6$	1.08	0.922	4000±200
AC	$n=2$	1.88	27.9	1.95±0.15
AC	$n=3$	1.52	19.6	5.02±0.18
AC	$(Me_2Si)_6$	1.45	18.0	22.7±0.5
AC	$n=4$	1.33	15.2	5.52±0.4
AC	$n=6$	1.08	9.45	19.1±2.5
BP	$n=2$	1.88	25.1	1.72±0.20
BP	$n=4$	1.33	12.4	6.72±0.40

[a] Redox potentials vs. SCE in acetonitrile from Refs. [7,34,36]; E_T from 0,0 band of phosphorescence in methyltetrahydrofuran [34].
[b] CNA, $E_{red} = -1.58$ V, $E_T = 69.2$ kcal mol^{-1}; AC, $E_{red} = -2.14$ V, $E_T = 73.5$ kcal mol^{-1}; BP, $E_{red} = -1.83$ V, $E_T = 69.2$ kcal mol^{-1}.

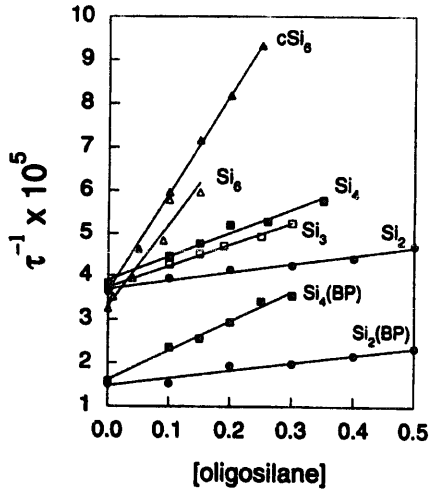

Fig. 3. τ^{-1} vs. [oligosilane] for quenching of acetophenone by disilane (Si_2), trisilane (Si_3), tetrasilane (Si_4), hexasilane (Si_6) and cyclic silane ($Me_2Si)_6$ (cSi_6). Data labeled by BP refer to quenching of benzophenone.

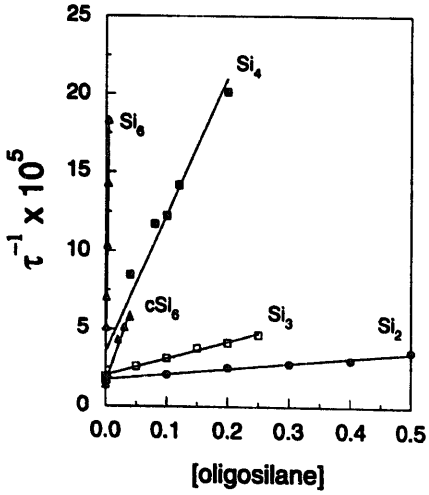

Fig. 4. τ^{-1} vs. [oligosilane] for quenching of *p*-cyanoacetophenone by disilane (Si_2), trisilane (Si_3), tetrasilane (Si_4), hexasilane (Si_6) and cyclic silane ($(Me_2Si)_6$ (cSi_6).

formed from the reaction of methyl ketones with silenes [37], produced directly or by silyl radical disproportionation. Additional products are observed, possibly associated with reactions of alkylsilyl and silyl radicals [11,38] with starting ketone, the solvent and self-reactions. The photomixtures were more complex with tetrasilane as quencher, since two sites are available for hydrogen abstraction and two different Si–Si bonds can cleave to give monosilanyl, disilanyl and trisilanyl fragments. For these reasons, no product studies were conducted with the hexasilane $Me_3Si(SiMe_2)_4SiMe_3$ as quencher. In addition, the identification and quantification of non-volatile pinacols and silylated pinacols hinged on the monitoring of the methyl proton signals of the photolysates by ^{1}H NMR spectroscopy. Thus the photoproducts of the trifluoroacetophenones were not determined.

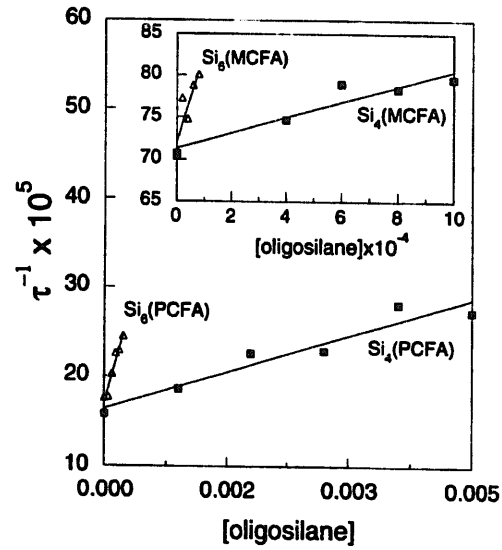

Fig. 5. τ^{-1} vs. [oligosilane] for quenching of *p*-chlorotrifluoroacetophenone (PCFA) by tetrasilane (Si_4) and hexasilane (Si_6); the disilane (Si_2) is omitted because of the much higher concentrations (≥ 0.1 M) needed to observe quenching. Inset shows τ^{-1} vs. [oligosilane] for quenching of *m*-chlorotrifluoroacetophenone (MCFA) by tetrasilane (Si_4) and hexasilane (Si_6).

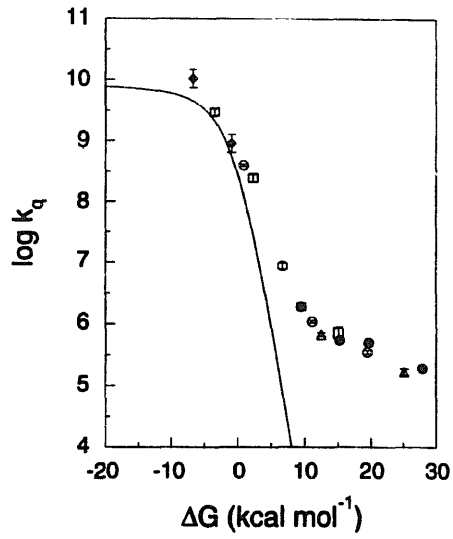

Fig. 6. Plot of log k_q vs. ΔG_{et} for phosphorescence quenching of acetophenone (●), benzophenone (△), *p*-cyanoacetophenone (○), *p*-chlorotrifluoroacetophenone (□) and *m*-chlorotrifluoroacetophenone (◆) in benzene.

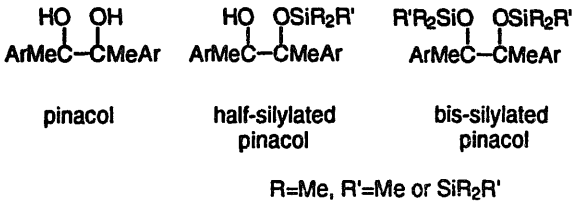

In the case of acetophenone with disilane or tetrasilane as quencher, the major products were diastereomeric acetophenone pinacols in a 1 : 1 ratio. These were identified by comparison of their retention times and GC-MS data with those of an authentic sample. Among the minor products were mono(trimethylsilyl) pinacols (1 : 1 diastereomers). With the tetrasilane, the mono(pentamethyldisilanyl) and mono(heptamethyltrisilanyl) pinacols were also formed.

Diastereomeric pinacols (1 : 1 mixture) were also major photoproducts of *p*-cyanoacetophenone and disilane in benzene. Both diastereomers precipitated from solution on concentration of the photolysate and sometimes during photolysis. Identification was by comparison of the mixture m.p. with that of an authentic sample and by comparison of the NMR spectral data. Gravimetric analysis gave a 6.4% yield. From MPLC of the photolysate, mono(trimethylsilyl) and bis(trimethylsilyl) pinacols were isolated in 0.7% and 0.4% yields together with 87% of unreacted ketone. The monosilylated pinacol was identified by comparison of its ^{1}H NMR data with those of an authentic sample, and the bis-silylated pinacol was characterized spectroscopically, including HR MS. The product yields are based on the stoichiometry of the reaction, i.e. 2 mmol ketone are consumed per millimole of product formed. GC analysis of a separate photolysis showed that the amounts of ketone and disilane consumed were 0.14 mmol and 0.19 mmol respectively.

Photolysis of *p*-cyanoacetophenone and tetrasilane in benzene gave, as the major products, a mixture of permethylated bis(polysilanyl) pinacols in an approximate 1 : 1 ratio of the diastereomers. ^{1}H NMR analysis of the photolysates showed the unsilylated pinacol to be only a very minor photoproduct, and the half-silylated pinacols were not detected. The non-volatile bis(polysilanyl) pinacols were isolated as a mixture by liquid chromatography. Although the similarity in the structures of these products precluded separation, unambiguous characterization of the mixture by spectroscopic methods proved feasible. The ^{13}C (APT) NMR spectra showed characteristic clusters, each of five peaks, for $\underline{C}H_3$–C centered at $\delta = 23.6$, quaternary $\underline{C}$–O centered at $\delta = 81.5$ and quaternary aromatic $\underline{C}$–CN centered at $\delta = 110.6$. Also present were two sets of upfield methyls attached to silicon, the aromatic CH, quaternary CN and quaternary aromatic carbons attached to benzylic C–O. These assignments were confirmed by heterocorrelated two-dimensional (HETCOR) NMR, which specifically related $\underline{C}H_3$–C in the ^{13}C NMR spectrum to two clusters of $C\underline{H}_3$ protons centered at $\delta = 1.35$ and $\delta = 1.78$ in the ^{1}H NMR spectrum, corresponding closely in chemical shift to the methyl protons of the above bis(trimethylsilyl) pinacol. On the other hand, the ^{13}C NMR spectrum was similar to that of authentic pinacol. IR spectroscopy of the isolated bis(polysilanyl) pinacol mixture showed no OH. The mono(trimethylsilyl) pinacol showed characteristic signals in the ^{1}H NMR spectrum for $C\underline{H}_3$–C at $\delta = 1.38$ and $\delta = 1.51$, and the latter signal was not present in photolysates prior to chromatography. ^{1}H NMR analysis of the photolysate showed the bis(polysilanyl) pinacols to be formed in 10% yield, with only traces of unsilylated pinacol present at 40% conversion of ketone. GC analysis indicated approximately 60% unreacted ketone, and twice the amount of ketone was consumed as tetrasilane, i.e. 0.335 mmol vs. 0.173 mmol respectively.

The quantum yields of the major products were determined at half-quenching such that $\tau^{-1} = k_q[Q]$ where Q ≡ disilane or tetrasilane. In the case of the pinacols and half-silylated pinacols, the quantum yields were calculated on the basis of 1 mmol pinacol produced per 2 millieinstein of light absorbed. The quantum yields of bis-silylated pinacols assume 1 mmol product formed per 1 millieinstein absorbed, although an unknown fraction of product will be formed with the same stoichiometry as the unsilylated and half-silylated pinacols. Thus the quantum yields of bis-silylated pinacols are a lower limit, and may be twice the reported value. At half-quenching of acetophenone with $Me_3SiSiMe_3$, Φ(pinacol) = 0.039 and Φ(half-silylated pinacol) = 0.0040. For *p*-cyanoacetophenone and $Me_3SiSiMe_3$, Φ(pinacol) = 0.019, Φ(monotrimethylsilyl pinacol) = 0.010 and Φ(bis-(trimethylsilyl) pinacol) = 0.0018; the quantum yield of disappearance of ketone was Φ_{dis}(ketone) = 0.062, while Φ_{dis}(disilane) = 0.086. For *p*-cyanoacetophenone and $Me_3Si(SiMe_2)_2SiMe_3$, Φ(pinacol) = 0.0058, Φ(monosilylated pinacol) ≈ 0.00, Φ(bis-silylated pinacols) = 0.020, Φ_{dis}(ketone) = 0.16 and Φ_{dis}(tetrasilane) = 0.082. Because tetrasilane is a more effective quencher than disilane, the concentrations for half-quenching of acetophenone and *p*-cyanoacetophenone were factors of 3 and 25 less respectively.

As described above, additional minor products are formed which may account for the low mass balances.

4. Discussion

The full curve in Fig. 6, which is from Rehm and Weller [10], corresponds to the theoretical log k_q vs. ΔG_{et} plot for electron transfer quenching of an excited state acceptor by a donor molecule according to the mechanism given in Scheme 1 [10]. In our study, the excited state electron acceptor A is the triplet aromatic ketone, the electron donor D is the ground state oligosilane, the rate constants k_{et} and k_{-et} are for forward and reverse electron transfer and the rate constants k_{diff} and k_{-diff} are for diffusional encounter and separation. The rate constant k_r denotes all processes for the deactivation of the CIRP or exciplex, such as back electron transfer to regenerate reactants and reaction of the triplet ketone with oligosilane to form products. The CIRP or exciplex produced on electron transfer is considered to be synonymous [35]. The solvent-separated ion radical pairs will not be intermediates, since the non-polar solvent benzene was used in our study, and thus the ΔG_{et} values are calculated from Eq. (1) [35,39] (see above). Application of the steady state approximation yields Eq. (2) for the rate constant for quenching k_q [10]

$$k_q = \frac{k_{diff}}{1 + (k_{-diff}/k_{et}) + (k_{-diff}/k_r)(k_{-et}/k_{et})} \quad (2)$$

Substituting $k_{-et}/k_{et} = e^{\Delta G_{et}/RT}$ and $k_{et} = k_0 e^{-\Delta G_{et}/RT}$ and taking $k_r = k_0 \sim 10^{11}$ s^{-1} (the maximum rate for forward or reverse electron transfer [10]) gives Eq. (3)

$$k_q = \frac{k_{diff}}{1 + (k_{diff}/Kk_r)(e^{\Delta G_{et}^{\ddagger}/RT} + e^{\Delta G_{et}/RT})} \quad (3)$$

In calculating k_q from Eq. (3) for benzene, $k_{-diff}/k_r = 0.12$ from $k_{-diff} = k_{diff}/K$ where k_{diff}(benzene) $= 1.0 \times 10^{10}$ M^{-1} s^{-1} and $K = 0.86 = k_{diff}/k_{-diff} = (4/3)\pi(N/1000)r^3$ with $r = 7$ Å, as prescribed by Rehm and Weller [10]. The free energy of activation ($\Delta G_{et}^{\ddagger}$) is expressed in terms of ΔG_{et} by the Rehm–Weller free energy relation [10] of Eq. (4)

$$\Delta G_{et}^{\ddagger} = \frac{\Delta G_{et}}{2} + \left[\left(\frac{\Delta G_{et}}{2}\right)^2 + (\Delta G_{et}^{\ddagger}(0))^2\right]^{1/2} \quad (4)$$

where the reorganization energy or "intrinsic barrier" $\Delta G^{\ddagger}(0) = 2.4$ kcal mol^{-1} (acetonitrile).

The full curve in Fig. 6 is not fitted to the experimental data using $\Delta G^{\ddagger}(0)$ as an adjustable parameter. With the oligosilanes as σ electron donors, significant Si–Si bond weakening is expected in the CIRP, which may result in an increase in the reorganization energy so that $\Delta G^{\ddagger}(0) > 2.4$ kcal mol^{-1}, although our use of benzene as solvent may be expected to exert an opposite effect [40]. An increased $\Delta G^{\ddagger}(0)$ may account for the apparent broadening [41] of the curved intermediate region of log k_q vs. ΔG_{et} (Fig. 6). Coupled with a shift in the intrinsic E_{ox} and, hence, ΔG_{et} to more negative values, as suggested by Alberti et al. [11] in the light of the irreversible electrochemical oxidations, a better fit of our data to theory would be obtained. Whether the electron transfer from oligosilanes results in Si–Si bond dissociation in the CIRP is debatable. CIDNP studies of electron transfer from disilane to quinone triplets indicate that the ion radical pair Me_3Si–$SiMe_3^+Q^{\cdot -}$ with an intact Si–Si bond has a significant lifetime [12]. Back electron transfer to regenerate reactants via a similar intermediate (as a CIRP) is consistent with the low quantum yields of disappearance of *p*-cyanoacetophenone at half-quenching by tetrasilane. This donor–acceptor pair falls within the approximately linear, Arrhenius-type region of electron transfer in Fig. 6, where triplet quenching is predominantly by the mechanism given in Scheme 1, as discussed below.

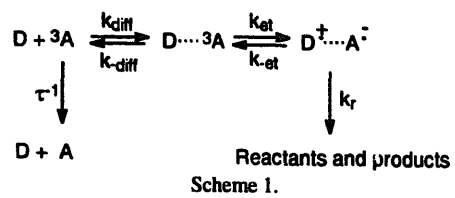

Scheme 1.

In the highly endergonic region of Fig. 6, strong deviations from the electron transfer mechanism in Scheme 1 are observed. Quenching in this region can be ascribed to the reaction of the oligosilane directly with the lowest triplet excited state of the ketone, rather than the electron transfer mechanism given in Scheme 1. The upward curvature in the free energy relationship of log k_q (Fig. 6) can be interpreted as a change in the mechanism [42] of quenching. As ΔG_{et} becomes less positive, the contribution to quenching by electron transfer from oligosilane to the triplet ketone acceptor rapidly increases in importance. The plot of log k_q vs. ΔG_{et} shows a nearly linear, Arrhenius-type behavior with a slope of the full curve approaching $1/2.3RT$ [10,41]. In this region, the electron transfer step given in Scheme 1 will be rate determining. With a further decrease in ΔG_{et} to negative values, the free energy relationship of Fig. 6 begins to level off in the intermediate region. Such a curvature of a free energy relation typically means a change in the rate-determining step [42]. In the case of quenching by oligosilane, the rate-determining step shifts from electron transfer in Scheme 1 to become diffusion controlled with the formation of the encounter complex as the rate-limiting step. Extending the Fig. 6 plot to $\Delta G_{et} < -7$ kcal mol^{-1} utilizing our experimental method will be difficult because of the dearth of ketone acceptors having $E_{red} > -1.3$ V, $E_T > 69$ kcal mol^{-1}, measurable phosphorescence and triplet lifetimes greater than 100 ns in fluid solution.

The formation of pinacol and/or silylated pinacol products during the quenching of *p*-cyanoacetophenone and acetophenone by $Me_3SiSiMe_3$ and $Me_3Si(Me_2Si)_2SiMe_3$ can be discussed within the context of Scheme 2. Two mechanisms are possible for the formation of pinacols:

1. C–H homolysis with the transfer of a hydrogen atom directly in the n,π^* triplet excited state of the aromatic ketone;
2. electron transfer to generate an ion radical pair followed by proton transfer.

Likewise, silylated pinacols can be formed by S_H2 transfer of silyl radicals directly in the triplet excited state of the ketone or by heterolysis of an Si–Si bond with the transfer of silylenium ions. Cross-recombination of ketyl and silylated ketyl radicals would be expected to produce half-silylated pinacols.

The quantum yields at half-quenching show that pinacols are the major products of *p*-cyanoacetophenone and acetophenone plus disilane $Me_3SiSiMe_3$ as quencher, and acetophenone plus tetrasilane $Me_3Si(Me_2Si)_2SiMe_3$ as quencher. The pinacols are probably formed via direct hydrogen abstraction by the triplet ketone from the oligosilane (Scheme 2), since only a small contribution to quenching would be expected by the strongly endergonic electron transfer mechanism. The increased importance of quenching by electron transfer in the case of *p*-cyanoacetophenone and tetrasilane in Fig. 6 is accompanied by a corresponding change in product distribution to favor heavily the bis-silylated pinacol over the unsilylated pinacol, which is observed as only a very minor product. This change in product ratio can reasonably be explained in terms of Si–Si σ bond weakening with the displacement of the silylenium ion by the ketyl anion radical in the CIRP. Such a change in the mechanism from hydrogen atom transfer to silylenium displacement would be consistent with the upward curvature of the free energy relation of Fig. 6.

In the highly endergonic region of Fig. 6, quenching can be ascribed to hydrogen atom abstraction and possibly S_H2 displacement. In most of these cases, the rate constants k_q (Tables 2 and 3) are less than or comparable with those measured for hydrogen abstraction from cyclopentane, as judged from τ^{-1} for the decay of these ketones in cyclopentane as solvent (of the order of $10^6\,M^{-1}\,s^{-1}$ [43]). Although hydrogen atom transfer has a solid precedent as an n,π^* process of triplet ketones [34], with disilane as quencher no falloff is observed in the relative rates of quenching of CNA and PCFA π,π^* triplets compared with the n,π^* triplets of AC and BP, and the relative rates are 1.0 : 0.88 : 1.81 : 3.68 for AC : BP : CNA : PCFA. The smooth monotonic increase in k_q may be rationalized by hydrogen atom abstraction and S_H2 displacement via polarized transition states. In such cases, the rate constants for hydrogen atom abstraction by ketones may be expected to increase in proportion to I_p, E_{ox} or E_{red}, or ΔG_{et} [44,45].

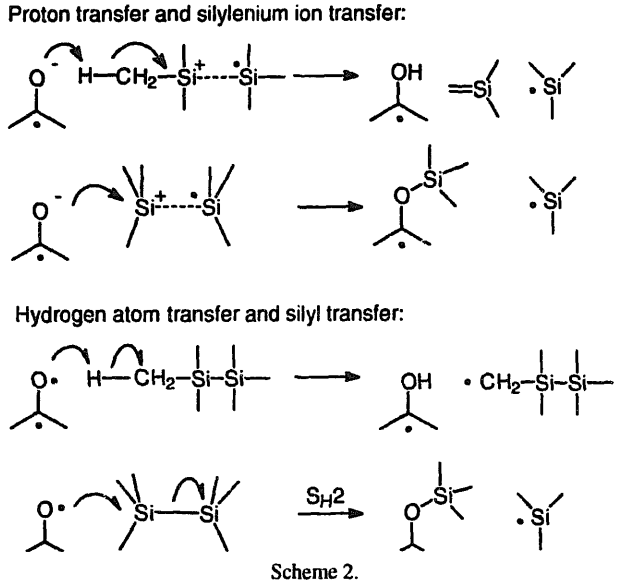

Scheme 2.

Acknowledgements

Financial support of this work by a Research Opportunity Award from Research Corporation (M.G.S.), NSF (CHE-9407036, M.G.S.; CHE-9313944, J.M.H.) and the College of Arts and Sciences, Marquette University (M.G.S.) is gratefully acknowledged.

References

[1] M.G. Steinmetz, Chem. Rev. 95 (1995) 1527.
[2] K.A. Horn, A.A. Whitenack, J. Phys. Chem. 92 (1988) 3875.
[3] T. Karatsu, H. Kobayashi, E. Shinkai, A. Kitamura, Chem. Lett. (1992) 2131.
[4] Y. Nakadaira, A. Sekiguchi, Y. Funada, H. Sakurai, Chem. Lett. (1991) 327.
[5] Y. Nakadaira, N. Komatsu, H. Sakurai, Chem. Lett. (1985) 1781.
[6] S. Fukuzumi, T. Kitano, K. Mochida, Chem. Lett. (1989) 2177.
[7] W.G. Boberski, A.L. Allred, J. Organomet. Chem. 88 (1975) 65.
[8] H.S. Plitt, J.W. Downing, M.K. Raymon, V. Balaji, J. Michl, J. Chem. Soc., Faraday Trans. 90 (1994) 1653.
[9] R.D. Miller, J. Michl, Chem. Rev. 89 (1989) 1359.
[10] D. Rehm, A. Weller, Ber. Bunsenges. Phys. Chem. 73 (1969) 834; Israel J. Chem. 8 (1970) 259.
[11] A. Alberti, S. Dellonte, C. Paradisi, S. Roffia, G.F. Pedulli, J. Am. Chem. Soc. 112 (1990) 1123.
[12] M. Igarashi, T. Ueda, M. Wakasa, Y. Sakaguchi, J. Organomet. Chem. 421 (1991) 9.
[13] P.J. Wagner, H.M.H. Lam, J. Am. Chem. Soc. 102 (1980) 4167.
[14] K.T. Dishart, R. Levine, J. Am. Chem. Soc. 78 (1956) 2268.
[15] P.J. Wagner, E.J. Siebert, J. Am. Chem. Soc. 103 (1981) 7329.
[16] H. Gilman, R.A. Tomasi, J. Org. Chem. 28 (1963) 1651.
[17] H. Gilman, G.D. Lichtenwalter, J. Am. Chem. Soc. 80 (1958) 608.
[18] H. Gilman, R.L. Harrell, J. Organomet. Chem. 5 (1966) 201.
[19] M. Kumada, M. Ishikawa, J. Organomet. Chem. 1 (1963) 153.
[20] M. Kumada, M. Yamaguchi, Y. Yamamoto, J.-I. Nakajima, K. Shiina, J. Org. Chem. 21 (1956) 1264.
[21] H. Gilman, S. Inoue, J. Org. Chem. 29 (1964) 3418.
[22] Y.-P. Sun, J. Michl, J. Am. Chem. Soc. 114 (1992) 8186.
[23] J.H. Markgraf, T.A. Newton, J. Chem. Educ. 56 (1979) 344.
[24] A. Furstner, R. Csuk, C. Rohrer, H. Weidmann, J. Chem. Soc., Perkin Trans. 1 (1988) 1729.
[25] E.J. Corey, B.B. Snider, J. Am. Chem. Soc. 94 (1972) 2549.
[26] M.G. Steinmetz, C. Yu, L. Li, J. Am. Chem. Soc. 116 (1995) 932.
[27] H.E. Zimmerman, Mol. Photochem. 3 (1971) 281.
[28] C.G. Hatchard, C.A. Parker, Proc. R. Soc. London, Ser. A 235 (1956) 518.

[29] T.R. Viegut, P.J. Pisano, J.M. Mueller, M.J. Kenney, J.M. Hossenlopp, Chem. Phys. Lett. 195 (1992) 568.
[30] I_p for $Me_3Si(SiMe_2)_{n-2}SiMe_3$ ($n=2$–4) and $(Me_2Si)_6$: H. Bock, W. Ensslin, Angew. Chem. Int. Ed. Engl. 10 (1971) 404.
[31] I_p for hexasilane ($n=6$) calculated from the charge transfer band with tetracyanoethylene ($h\nu_{ct}=7.70$ eV) utilizing $h\nu_{ct}(eV)=0.771I_p-3.716$: V.F. Traven, V.N. Karel'skii, V.F. Donyagina, E.D. Babich, B.I. Stepanov, V.M. Vdovin, N.S. Nametkin, Dokl. Akad. Nauk SSSR 224 (1975) 837.
[32] A.A. Gorman, C.T. Parekh, M.A.J. Rogers, P.G. Smith, J. Photochem. 9 (1978) 11. J.B. Guttenplan, S.G. Cohen, J. Am. Chem. Soc. 94 (1972) 4040. J.B. Guttenplan, S.G. Cohen, Tetrahedron Lett. (1972) 2163. D. Griller, J.A. Howard, P.R. Marriot, J.C. Scaiano, J. Am. Chem. Soc. 103 (1981) 612.
[33] F.D. Lewis, T.A. Hilliard, J. Am. Chem. Soc. 94 (1972) 3852.
[34] P.J. Wagner, R.J. Truman, A.E. Puchalski, R. Wake, J. Am. Chem. Soc. 108 (1986) 7727.
[35] A. Weller, Z. Phys. Chem. N.F. 133 (1982) 93.
[36] H. Watanabe, K. Yoshizumi, T. Murakao, M. Kato, Y. Nagai, T. Sato, Chem. Lett. (1985) 1683.
[37] W.J. Leigh, C.J. Bradaric, G.W. Sluggett, J. Am. Chem. Soc. 115 (1993) 5332.
[38] C. Chatgilialoglu, Chem. Rev. 95 (1995) 1229.
[39] B.R. Arnold, S. Farid, J.L. Goodman, I.R. Gould, J. Am. Chem. Soc. 118 (1996) 5482.
[40] G.B. Schuster, Adv. Electron Transfer Chem. 1 (1991) 163.
[41] F. Scandola, V. Balzani, G.B. Schuster, J. Am. Chem. Soc. 103 (1981) 2519.
[42] F. Ruff, I.G. Csizmadia, Organic Reactions, Equilibria, Kinetics and Mechanism, Stud. Org. Chem. 50, Elsevier, 1994, pp. 173–174.
[43] P.J. Wagner, R.J. Truman, J.C. Scaiano, J. Am. Chem. Soc. 107 (1985) 7093.
[44] L. Cermenati, M. Freccero, P. Venturello, A. Albini, J. Am. Chem. Soc. 117 (1995) 7869.
[45] Y.M.A. Naguib, C. Steel, S.G. Cohen, M.A. Young, J. Phys. Chem. 91 (1987) 3033.